Coupled dynamics of atoms and radiation-pressure-driven interferometers

D. Meiser and P. Meystre
Department of Physics, The University of Arizona, 1118 East 4th Street, Tucson, Arizona 85721, USA
(Received 28 November 2005; published 21 March 2006)

We consider the motion of the end mirror of a cavity in whose standing-wave mode pattern atoms are trapped. The atoms and the light field strongly couple to each other because the atoms form a distributed Bragg mirror with a reflectivity that can be fairly high. We analyze how the dipole potential in which the atoms move is modified due to this back action of the atoms. We show that the position of the atoms can become bistable. These results are of a more general nature and can be applied to any situation where atoms are trapped in an optical lattice inside a cavity and where the back action of the atoms on the light field cannot be neglected. We analyze the dynamics of the coupled system in the adiabatic limit where the light field adjusts to the position of the atoms and the light field instantaneously and where the atoms move much faster than the mirror. We calculate the sideband spectrum of the light transmitted through the cavity and show that these spectra can be used to detect the coupled motion of the atoms and the mirror.

DOI: 10.1103/PhysRevA.73.033417 PACS number(s): 32.80.Pj, 42.50.Vk, 45.90.+t

I. INTRODUCTION

In recent years the coupling of the light field inside an optical resonator to the mechanical motion of the end mirrors [1–3] has received renewed attention due to several developments. The improved capabilities to micromachine submicrometer-sized mechanical structures with well-defined mechanical and optical properties enable the creation of movable mirrors with small damping whose motion is strongly affected by the radiation pressure due to the light field inside an optical cavity. The coupled nonlinear dynamics found in those systems is very rich [4,5] and is relevant for systems as large as gravitation-wave antennas [6–8] down to micromachined cavities [4]. The radiation pressure force can be used to isolate the mechanical motion of the end mirror from the seismic background [2]. Recently, schemes for active cooling of mirrors with radiation pressure have been proposed [9] and implemented [10–12]. It is expected that with these methods cooling of the mirror motion to its quantum-mechanical ground state will be possible and that the quantized motion of a macroscopic object, including nonclassical states of motion and squeezing, can be studied this way [13–15]. Also, the mirror could become entangled with the light field [16], and questions related to position measurements near the quantum limit can be addressed. In the classical regime the mirror motion can exhibit instabilities, self-sustained oscillations [4], and chaos due to the retardation of the electromagnetic field in certain cases.

From a theoretical point of view, radiation-pressure-driven cavities offer many challenges and opportunities. These systems provide excellent testing grounds for theories of systems with delay [8,17]. Furthermore, quantizing the light field is a nontrivial question in principle for time-dependent boundary conditions [18].

In this paper we extend the study of radiation-pressure-driven interferometers to the case where atoms are trapped in the optical dipole potential generated by the standing-wave light field inside the cavity (see Fig. 1). In this system the atoms, light field, and mirror interact with each other on an equal footing in the most general case. We derive the equations governing this system from first principles. Treating the motion of the mirror as well as the light field classically, we show that in many cases of interest the motion of the atoms can also be described classically. We restrict ourselves to those situations in this paper. Our key result is that, surprisingly if one considers the complexity of the problem, it is possible to develop an effective theory that captures many of the aspects of the system and is amenable to a fairly simple analysis under moderate assumptions. The key observation is that the effect of the atoms on the light field can be represented by an effective mirror whose reflection and transmission coefficients can be calculated from the self-consistently determined atomic density distribution. As we will discuss the atoms naturally arrange themselves in a configuration corresponding to a Bragg mirror of maximum reflectivity for a given number of atoms [19]. Thus, all degrees of freedom of the atoms collapse into a single coordinate describing the position of this fictitious mirror.

The collective back action of the atoms, as described by what we may call the "atom mirror," strongly affects the light field. Thus the atoms qualitatively change the potential in which they move themselves. Furthermore, because of the modifications of the radiation pressure force, they also influence the mirror motion.

As a consequence of the back action on the light field the potential wells in which the atoms sit become narrower and for certain mirror positions exhibit two local minima per half optical wavelength, i.e., the atomic position becomes bistable. The character of the bifurcation points where the single potential well branches off into two valleys can be modified by changing the cavity parameters, such as, e.g., the reflectivities of the two end mirrors. In that way it is possible to choose which of the two valleys is the deeper one and accordingly in which direction the atoms will move. The two side valleys can also be made equally deep, in which case the branching point acts like an atomic beam splitter. We also show that the atomic motion can exhibit hysteresis, where the atoms move along different paths depending on the direction of motion of the mirror, giving rise to additional instabilities of the mirror motion.

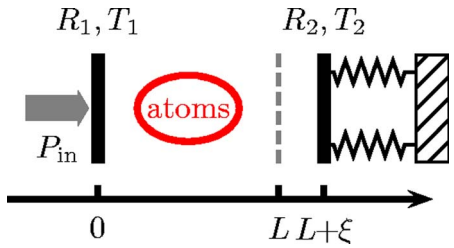

FIG. 1. (Color online) Schematic of atoms in a cavity with a movable mirror.

In this paper we consider only the adiabatic limit where the mirror moves slowly compared with the atoms, which in turn have a much slower response time than the intracavity light field. Even in that limit the coupled system exhibits a remarkably rich phenomenology that we illustrate by analyzing and discussing the modified dipole potential experienced by the atoms as well as the modified motion of the end mirror.

We propose to measure the sideband spectrum of the light transmitted through the cavity as a quantitative indicator of the coupled atom-mirror motion, as the coupling of the mirror motion to the atoms gives rise to unambiguous spectral signatures that should be within easy experimental reach.

This article is organized as follows. In Sec. II we describe the model for the coupled atom-mirror–field system and derive the basic dynamical equations. In Sec. III we consider the dynamics of the mirror with field and atoms following its motion adiabatically, and discuss several aspects of the atomic motion. In Sec. IV we calculate the spectrum of the light transmitted through the cavity and show that it can serve as a convenient probe of the coupled mirror-atom motion. Finally, Sec. V is a conclusion and outlook.

II. MODEL

The system under consideration is shown schematically in Fig. 1. Atoms are trapped in the standing-wave light field of a Fabry-Pérot cavity with one of its end mirrors allowed to move under the effect of radiation pressure and subject to a harmonic restoring force, ξ being the displacement of the mirror from its rest position. The cavity length offset L only gives rise to a shift of the resonances and we will set it to zero in all that follows.

We measure all lengths in units of the vacuum wavelength of the light and all times in units of Ω_P^{-1}, where Ω_P is the oscillator frequency of the unperturbed moving mirror. The electrical fields are described in terms of their intensity integrated over the beam profile, i.e., in terms of power.

A. Atoms

Using $\hbar\Omega_P$ as the unit of energy and $\hbar k_0 = \hbar 2\pi/\lambda_0$ as the unit of momentum the free Hamiltonian of the atoms takes the form

$$\hat{H} = \int d^3x\, \hat{\psi}^\dagger(x)\left(-\frac{E_R}{4}\nabla^2 + \frac{U_0}{2}\hat{\psi}^\dagger(x)\hat{\psi}(x)\right)\hat{\psi}(x), \qquad (1)$$

where $\hat{\psi}$ and $\hat{\psi}^\dagger$ are the atomic field annihilation and creation operators. Our theory can easily be adapted to describe fermions or bosons although at the level of our present theory there are no significant effects due to the statistics of the atoms. For the sake of definiteness we nonetheless assume that the field operators in Eq. (1) satisfy bosonic commutation relations. The energy

$$E_R = \frac{(2\hbar k_0)^2}{2M\hbar\Omega_P}$$

with M the mass of the atoms is the two-photon recoil energy and

$$U_0 = \frac{E_R a}{\lambda_0 \pi}$$

with a the s-wave scattering length is the interaction strength between the atoms describing s-wave collisions.

We assume that the atoms can be approximated as two-level atoms with transition frequency ω_a and we treat their interactions with the light field in the dipole and rotating-wave approximations. We consider only one state of polarization of the light field and describe this component by a scalar field. Furthermore we assume that the intracavity light field of frequency ω_L is far detuned from the atomic transition, $|\Delta| \equiv |\omega_L - \omega_a| \gg \Omega_R, \gamma$. Here Ω_R is the Rabi frequency of the transition and γ is its linewidth. Then we can adiabatically eliminate the upper state and, choosing the z axis along the direction of propagation of the light field, the interaction between light field and atoms is given by the dipole potential

$$\hat{H}_{\text{int}} = g\int d^3x\, \psi^\dagger(x)\psi(x)|E(z)|^2|u_\perp(x,y;z)|^2 \qquad (2)$$

where

$$g = \frac{2}{\hbar^2 c\epsilon_0 \lambda_0^2 \Omega_P}\frac{\wp^2}{\Delta}, \qquad (3)$$

where $\wp$ is the electric dipole moment along the polarization direction of the laser field and the electrical field has been split into a part varying along the cavity axis z and a transverse profile $u_\perp(x,y;z)$ assumed to be normalized to unity,

$$\int dx\, dy |u_\perp(x,y;z)|^2 = 1, \qquad (4)$$

for every z. For simplicity we assume in the following that the z dependence of $u_\perp$ along the atomic cloud can be neglected. We further assume that the light field is red detuned, $\Delta < 0$, so that the atoms are attracted to the intensity maxima.

The standing wave that forms in the cavity results in an optical lattice potential. We assume that its wells are very deep, i.e., $g|E_0|^2 \gg E_R$, where E_0 is the amplitude of the standing wave. In the language of condensed matter physics we assume that the atoms are deeply in the Mott insulator regime [20]. It is then a good approximation to assume that every site has a specific number of atoms in the ground state of the harmonic oscillator potential representing the lattice at that site. Due to the back action of the atoms on the light field the distance between the lattice sites is smaller than $\lambda_0/2$, a point to which we return shortly.

The interaction between atoms only gives rise to a constant energy shift. Its influence on the localized wave functions is irrelevant since all that will be required in the following is that the atomic density at every site is localized within much better than an optical wavelength. The order of magnitude of the localization is given by the oscillator length at a single lattice site,

$$a_{\mathrm{osc},z} = \left(\frac{\pi w^2 E_R}{4g|E_0|^2 k_0^2} \right)^{1/4} \tag{5}$$

along the cavity axis and

$$a_{\mathrm{osc},\perp} = \left(\frac{\pi w^4 E_R}{4g|E_0|^2} \right)^{1/4} \tag{6}$$

in the transverse direction. For typical laser powers and detunings the oscillator length is roughly 10–100 times smaller than the optical wavelength. The oscillator frequencies are

$$\omega_{\mathrm{osc},z} = \sqrt{\frac{g|E_0|^2 k_0^2 E_R}{\pi w^2}} \tag{7}$$

for oscillations along the cavity axis and

$$\omega_{\mathrm{osc},\perp} = \sqrt{\frac{g|E_0|^2 E_R}{\pi w^4}} \tag{8}$$

for oscillations in the transverse direction. The parameters that we are interested in are such that the oscillator length in the longitudinal direction is much smaller than an optical wavelength and the oscillator length in the transverse direction is much smaller than the beam waist. Since the beam is typically much wider than an optical wavelength the atoms can be thought of as forming a stack of pancake-shaped disks.

We consider an optical lattice with N sites occupied by n atoms each. Due to the phase shift suffered by the light upon propagation through each atomic sheet the lattice sites move closer together, the self-consistent period of the resulting lattice being determined later on. If the temperature of the atoms is far below the oscillator energy, we are justified in neglecting thermal excitations. If the atoms start in the lattice ground state, the atomic motion is then reduced to the motion of a Gaussian wave packet in a slowly changing harmonic potential, a situation that is well described by the classical dynamics of the atomic center of mass.

Because atoms at different sites see the exact same potential at all times they will be at the same displacement from their respective local minima given that they started at the bottom of their respective potential wells. Therefore it is possible to describe the atomic motion in terms of a single coordinate z_a, the position of each atom modulo the lattice period.

B. Moving mirror

The mirror motion is described by the Newtonian equation of motion

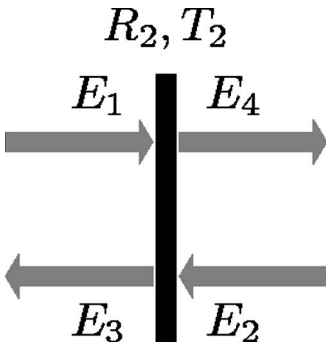

FIG. 2. Field geometry at movable mirror.

$$\ddot{\xi} + \Gamma \dot{\xi} + \xi = \frac{F_{\mathrm{RP}}}{m_P \Omega_P^2 \lambda_0} \equiv \alpha c F_{\mathrm{RP}}, \tag{9}$$

where c is the speed of light, Γ^{-1} is the mechanical quality factor of the mirror, F_{RP} is the radiation pressure force, and

$$\alpha^{-1} = m_P \Omega_P^2 \lambda_0 c$$

is a power characteristic of the mirror. The electromagnetic field is treated classically and from Fig. 2 we read off that

$$F_{\mathrm{RP}} = \frac{1}{c}(|E_1|^2 + |E_3|^2 - |E_4|^2 - |E_2|^2) = \frac{2|R_2|^2|E_1|^2}{c} \tag{10}$$

where we have used that in our situation $E_2 \equiv 0$.

C. Light field

We now turn to the back action of the atoms on the light field. The influence of the cavity mirrors will be considered in the next section.

It is well known [21] that for large detuning, optically driving the atoms results in the polarization

$$P = \frac{-2\wp^2}{\hbar \Delta} \hat{\psi}^\dagger \hat{\psi} E u_\perp \tag{11}$$

leading to the inhomogeneous optical field propagation equation

$$\nabla^2 (E u_\perp) + k_0^2 (E u_\perp) = \chi |\psi|^2 (E u_\perp) \tag{12}$$

where in our units the polarizability is given by

$$\chi = \frac{2\mu_0 \Omega_P}{\hbar} \frac{\wp^2 \omega_L^2}{\Delta}. \tag{13}$$

In principle, the shape of the transverse profile $u_\perp$ is the result of the complicated dynamics resulting from the repeated propagation of the light field through the cavity and its interaction with the complicatedly structured dielectric constituted by the atoms. A complete description of these processes is beyond the scope of this paper. We instead adopt the point of view that $u_\perp$ has been established in some way and is assumed to be known. We therefore describe it an effective manner and eliminate it from the theory.

Specifically, we assume that $u_\perp$ varies slowly with z, $|\partial u_\perp / \partial z| \ll |k_0 u_\perp|$, so that we can neglect its derivatives with

respect to z. Then, after dividing by $Eu_\perp$ to separate the variables, we have from the wave equation

$$\frac{\partial^2 E(z)}{\partial z^2} + k_0^2 E(z) = \beta^2(z) E(z) \tag{14}$$

where $\beta(z)$ is determined for every z by the eigenvalue problem

$$\chi|\psi(x,y,z)|^2 u_\perp(x,y;z) - \nabla_\perp^2 u_\perp(x,y;z) = \beta^2(z) u_\perp(x,y;z). \tag{15}$$

In principle this formula solves our problem since it expresses the propagation equation for E in terms of ψ and $u_\perp$ independently of how the latter was obtained. In order to obtain a more transparent formula we multiply Eq. (15) by $u_\perp^*$, integrate over x and y, and after a partial integration we find

$$\begin{aligned}\beta^2(z) &= \chi \int dx\, dy |u_\perp(x,y,z)|^2 |\psi(x,y,z)|^2 \\ &\quad + \int dx\, dy [\nabla_\perp u_\perp^*(x,y;z)] \cdot [\nabla_\perp u_\perp(x,y;z)] \\ &\equiv \chi \overline{|\psi(z)|^2} + k_\perp^2(z),\end{aligned} \tag{16}$$

ending up with the intuitively appealing equation

$$\frac{\partial^2 E(z)}{\partial z^2} + [k_0^2 - k_\perp^2(z)] E(z) = \chi \overline{|\psi(z)|^2} E(z), \tag{17}$$

where $\overline{|\psi(z)|^2}$ can be interpreted as the density distribution averaged over the transverse beam profile. In the following we neglect the reduction of the wave vector k_0 due to the finite extent of the beam in the transverse direction, an approximation valid if the beam is not too strongly focused.

For the situation at hand $\overline{|\psi(z)|^2}$ is readily found, since the wave function of the harmonic oscillator factorizes into a z-dependent part and a transverse part. As discussed above the atomic density distribution is much narrower than the beam waist w. Hence we find, assuming a Gaussian beam profile,

$$\overline{|\psi(z)|^2} = \frac{1}{\pi w^2} |\psi_z(z)|^2, \tag{18}$$

where $\psi_z(z)$ is the z-dependent factor of the oscillator wave function of the atoms.

Equation (17) allows us to determine the effect of the atoms on the light field. The basic idea is to replace the entire configuration of atoms by a fictitious "atom mirror" at some position z_a and hence to describe them in terms of a pair of effective reflection and transmission coefficients. The period of the self-consistent lattice automatically satisfies the Bragg condition. Due to the self-consistency requirement this is even true for a lattice with nonuniform filling; see Ref. [19] for more details. (Parenthetically, this means that we can take into account an external trapping potential through an appropriate choice of effective N and n. The thermal motion of the atoms will lower the reflectivity of the atom mirror and could be taken into account through a Debye-Waller factor.) All that remains to do to describe the effect of the atoms on the light field is to determine the transmission and reflection coefficient T and R of the atom mirror. A schematic of the situation is shown in Fig. 3.

Consider first a single atomic sheet. Making use of the fact that the atoms are localized in the z direction to a much narrower region than an optical wavelength, we readily find the transmission and reflection coefficients

$$T_s = \sqrt{\frac{1}{1+\Lambda^2}} e^{i\phi}, \tag{19}$$

$$R_s = i\sqrt{\frac{\Lambda^2}{1+\Lambda^2}} e^{i\phi}, \tag{20}$$

by matching boundary conditions at the atom sheet. Here

$$\phi = -\arctan \Lambda \tag{21}$$

is the phase shift suffered by light upon transmission through the sheet of atoms and we have introduced the parameter

$$\Lambda = \frac{n\chi}{2\pi k_0 w^2} \tag{22}$$

for notational convenience. Equation (21) allows us to determine the self-consistent period of the optical lattice. Due to the interaction between the light field and the atoms the period of the optical lattice is reduced to

$$d = \frac{\pi - 2\phi}{k_0}. \tag{23}$$

The entire lattice of atoms can be considered as a periodically stratified dielectric medium. Its total reflection and transmission coefficients are readily found using standard methods of the optics of dielectric films [19,22]. In essence, one can find the transfer matrix of a unit cell of the lattice from the transmission and reflection coefficient Eqs. (20) and (19). The transfer matrix of the entire lattice is then the Nth power of the transfer matrix of the unit cell. This can be done in closed form using Chebyshev polynomials since we neglect scattering losses and therefore the transfer matrix of the unit cell is unimodular. From the total transfer matrix the total reflection and transmission coefficients are extracted as [1]

$$R = \frac{-i\Lambda N e^{2i\phi}}{1 - i\Lambda N}, \tag{24}$$

$$T = \frac{e^{2i\phi N}}{1 - i\Lambda N}. \tag{25}$$

An example of the transmission and reflection coefficients of such a lattice of atoms is shown in Fig. 4 for the case of

[1] Strictly speaking, Eq. (24) is the reflection coefficient for a wave propagating in the positive z direction with the reflection coefficient in the negative z direction differing by an additional phase $e^{4iN\phi}$. This phase is, however, immaterial for our discussion since it can be absorbed in a redefinition of z_a. The transmission coefficients for the two directions are exactly equal as they have to be for general reasons.

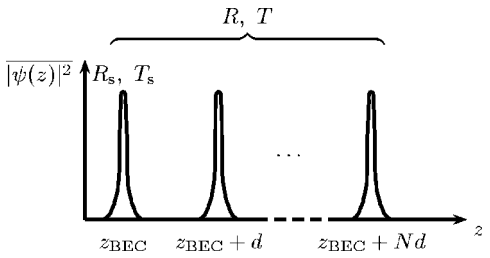

FIG. 3. Schematic of the Bragg mirror formed by the atoms. Each atomic sheet has a reflection and transmission coefficient R_s and T_s resulting in a total reflection and transmission coefficient R and T.

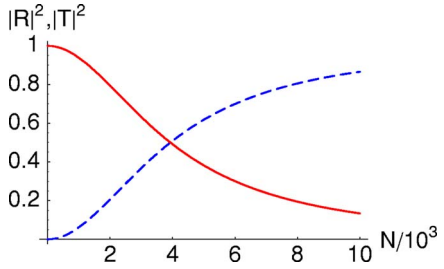

FIG. 4. (Color online) Reflection [(blue) dashed line] and transmission [(red) solid line] coefficients of an optical lattice consisting of ten ^{87}Rb atoms at every site as a function of the number of lattice sites for $\Delta=10^9\ s^{-1}$ and $w=10\lambda_0$ as obtained from Eqs. (24) and (25).

^{87}Rb. From the figure it is apparent that rather high reflectivities can be obtained in principle. One of the main experimental difficulties will be to achieve fairly high filling factors over many sites. Also, the high reflectivities in Fig. 4 were obtained by using a small beam waist and a fairly small detuning of around 100 linewidths. It should be noted that already fairly moderate reflection coefficients of the atoms of around 10% give rise to interesting effects as we discuss later in this paper. S. Slama *et al.* have recently reported Bragg reflection coefficients of the order of 30% [23]. (Note that the assumption of a constant and small beam waist is not as bad as might be expected, as the Gaussian-shaped atomic wave packets at every site act like lenses that constantly refocus the beam. A more detailed analysis of the spatial mode structure of the light field inside the cavity will be presented in future.)

In the following we consider the three representative cases of an empty cavity, a cavity containing atoms giving rise to an intermediate reflection coefficient of a few tens of a percent, and atoms with a reflection coefficient close to 1.

III. ADIABATIC DYNAMICS

We restrict ourselves to the limit where the motion of the moving mirror is extremely slow compared to the motion of the atoms, which is in turn very slow compared to the dynamics of the light field. For this to be true we must have $\Omega_P \ll \omega_{\mathrm{osc,z}}$ and $\omega_{\mathrm{osc,z}} \ll \kappa$ where κ is the linewidth of the cavity. This is the most relevant case for the typical systems currently available. The light field then follows the atoms adiabatically, so that both light field and atoms adjust instantaneously to any position of the moving mirror. We can then eliminate the atoms and the light field and express the radiation pressure force acting on the mirror in terms of the mirror position alone.

To obtain the effective radiation pressure force in presence of the atoms we observe that, given positions of the mirror and of the atoms, the equilibrium light field is determined by the boundary conditions at the fictitious atom mirror (see Fig. 5). The steady-state boundary conditions are found to be

$$\epsilon_1 = T_1 e^{ik_0 z}\sqrt{P_{\mathrm{in}}} + e^{2ik_0 z} R_1 \epsilon_2, \tag{26}$$

$$\epsilon_2 = R\epsilon_1 + T\epsilon_3, \tag{27}$$

$$\epsilon_3 = R_2 e^{2ik_0(L+\xi-z)}\epsilon_4, \tag{28}$$

$$\epsilon_4 = T\epsilon_1 + R\epsilon_3, \tag{29}$$

from which we obtain, e.g., for ϵ_4,

$$\epsilon_4 = \frac{-e^{ik_0 z_a}\sqrt{P_{\mathrm{in}}}TT_1}{RR_1 e^{2ik_0 z_a} + RR_2 e^{2ik_0(L+\xi-z_a)} - R_1R_2(R^2-T^2)e^{2ik_0(L+\xi)} - 1}. \tag{30}$$

From these fields we find the adiabatic dipole potential experienced by the atoms for a given displacement of the moving mirror as

$$V(z_a;\xi) = g|\epsilon_4+\epsilon_3|^2 = \frac{gP_{\mathrm{in}}|T_1T|^2[1+|R_2|^2-2|R_2|\sin 2k_0(L+\xi-z_a)]}{|RR_1e^{2ik_0z_a} + RR_2e^{2ik_0(L+\xi-z_a)} - R_1R_2(R^2-T^2)e^{2ik_0(L+\xi)} - 1|^2}. \tag{31}$$

The potential $V(z_a;\xi)$ is periodic with period $\lambda_0/2$ in both z_a and ξ directions. In the numerator we have, for $|R_2|$ close to 1, the well-known $\cos^2 k_0(L+\xi-z)$-type potential. Its minima are moving as the cavity end mirror is moving.

The effect of the denominator, which gives rise to a series of resonances, is somewhat less intuitive. If the reflection coefficient of the atoms is small their back action on the cavity field is weak and we see essentially the resonances of

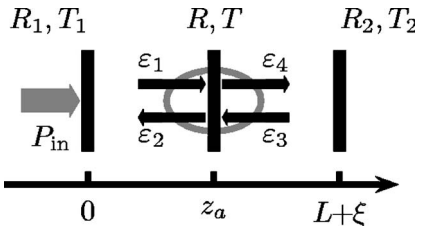

FIG. 5. Representation of the atoms as a mirror at z_a and illustration of the steady-state boundary conditions at z_a.

an empty Fabry-Pérot cavity: Whenever the distance between the two cavity mirrors is $(m+\frac{1}{2})\lambda_0/2$ with m an integer the field inside the cavity is very high and accordingly the dipole potential very deep.[2] Figure 6 shows how a small atomic reflectivity slightly distorts this type of potential. The zeros of the numerator are visible as dark diagonal lines and the nonzero regions are structured by the back action of the atoms on the light field.

The situation is qualitatively different if the reflection coefficient of the atoms is high (see Fig 7). In this case the dipole potential is deep whenever the atoms are in a position where they form a resonant cavity with one of the end mirrors. Interestingly, this typically gives rise to two potential minima per $\lambda_0/2$, resulting in two distinct modes of motion for the atoms: They can follow the moving mirror in the local minimum along diagonals in Fig. 7, or alternatively they can remain locked with the fixed mirror in the local minimum following vertical lines in Fig. 7. These two minima are actually already present for small atomic reflectivity, but only for a very narrow range of ξ values near $\xi \approx 0.25$.

The relative depth of the two local minima is determined by the reflectivities of the two end mirrors. The potential well closer to the mirror of higher reflectivity is deeper. As illustrated in Fig. 8 the system shows behavior reminiscent of an "avoided crossing" where the two resonances corresponding to the two modes of motion cross: In positions where the atoms would be on resonance with both mirrors the potential depth has a fairly narrow local maximum. The width of the potential barrier arising this way becomes smaller as the reflectivity of the atomic mirror increases. If the moving mirror sweeps through such a resonance, the atoms have to decide which branch of the potential valley to follow on the other side of the resonance.[3] Since we can decide which branch of the potential well is deeper by choosing the reflectivities of the end mirrors appropriately, we can select the mode of motion that the atoms will perform.

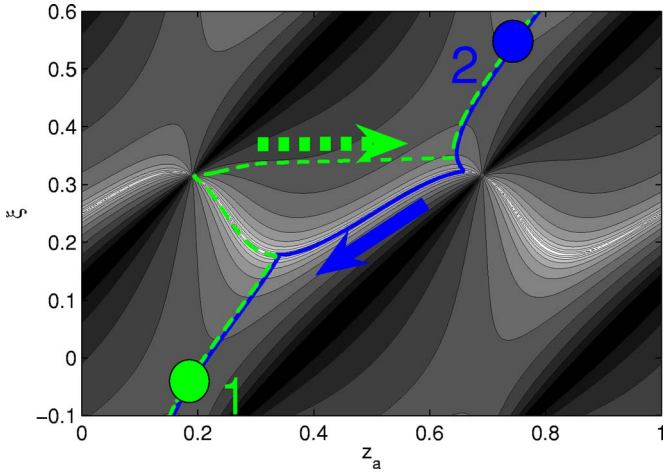

FIG. 6. (Color online) Dipole potential experienced by the atoms for $T_1=0.1$, $T_2=0.2$ and relatively high transmissivity of the atomic mirror, $T=0.90$. Here, and in the potential plots to follow, lighter regions are deeper in potential and the contour lines are drawn at logarithmic intervals for clarity and, as in the rest of this paper, all lengths are given in units of the wavelength of the injected light field. The (green) dashed line illustrates the path the atoms take when the mirror is moving starting at the (green) dot with the label 1 while the (blue) solid line shows the path the atoms take when the mirror moves back down starting at the (blue) dot labeled 2.

The adiabatic motion of the atoms is particularly interesting if the fixed mirror has the higher reflectivity. We discuss it in detail for the case of small atomic reflectivity. The trajectories of the local minima corresponding to the mirror moving in the positive, resp. negative ξ direction are drawn as a green dashed line and a blue solid line, respectively, in

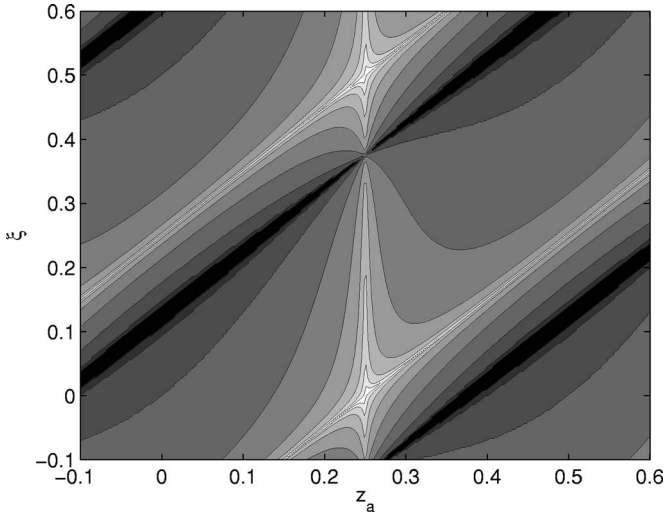

FIG. 7. Dipole potential for higher atomic reflectivity corresponding to $T=0.05$ and $T_1=0.2$, $T_2=0.1$. For this choice of reflectivities of the cavity end mirrors the potential well closer to the moving mirror is always deeper and, in contrast to Fig. 6, the atoms move on diagonals following the bottom of the potential well for both directions of the mirror motion.

[2]The additional $\lambda_0/4$ offset comes from a particular choice of phase of the reflection and transmission coefficients.

[3]The resonances act like beam splitters for the atoms and a more exact analysis should treat the motion of the atoms near these branching points quantum mechanically. Also one can easily convince oneself that atoms originally in neighboring potential wells can end up in the same potential well if they choose to go into different branches at a resonance. This provides one with the essential ingredients for an interferometer that can in principle operate in a massively parallel fashion. This problem will be studied in greater detail in the future.

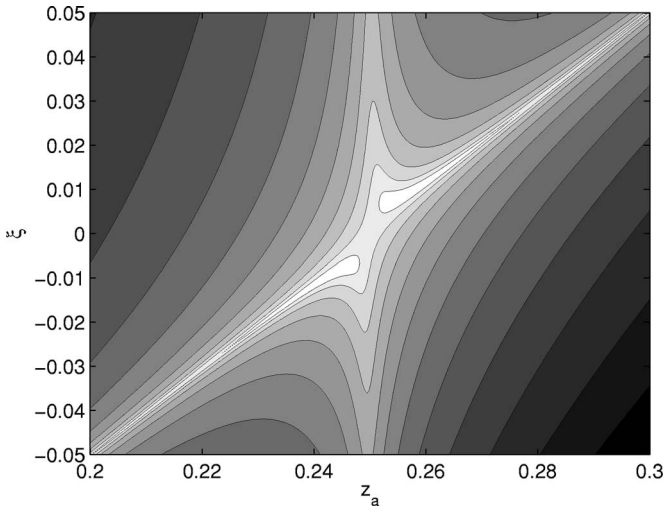

FIG. 8. Enlargement of the resonance region of Fig. 7, showing that the potential well corresponding to motion with the moving mirror is deeper than the one corresponding to the resonance with the fixed mirror, and explaining why the atomic motion is locked to the mirror motion. The figure also shows the avoided crossing of the dipole potential.

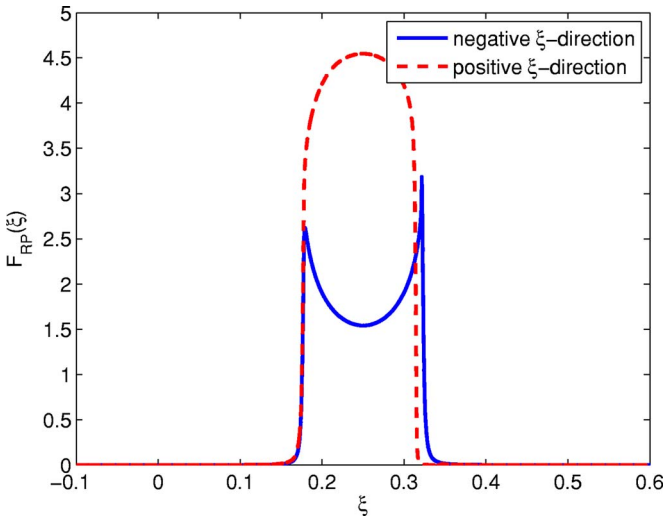

FIG. 9. (Color online) Radiation pressure force for the two directions of motion of the mirror. The atoms take the paths shown in Fig. 6 for the mirror moving in the positive and negative ξ directions, respectively. The difference in area of the two curves is a measure of the work performed on the moving mirror. All parameters as in Fig. 6.

Fig. 6. If the moving mirror starts in a region far off resonance, e.g., at the (green) dot labeled 1 in Fig. 6, there is only one potential minimum corresponding to the maximum of the numerator in the dipole potential. Moving in the direction of growing ξ the potential valley eventually reaches a branching point and the atoms follow it to the left toward the fixed mirror, since the potential well to the left is deeper if the fixed mirror has the higher reflectivity. Near the diagonal zero lines of the numerator the potential well becomes shallower and shallower until finally it ceases to provide a local minimum. The atoms "roll" to the second branch of the potential valley closer to the moving mirror and follow this local minimum until the system hits the next resonance, where this story repeats itself.

The atomic motion is totally different if the moving mirror moves in the negative ξ direction. Then the branch of the potential closer to the moving mirror provides a local minimum all the way and the atoms never move to the left branch [see the (blue) solid line in Fig. 6].

The motion of the atoms is similar for high atomic reflectivity. If the mirror is moving in the positive ξ direction the atoms turn left at every resonance into the vertical potential valley. Just before reaching the zero potential line they roll to the right and fall into the diagonal valley. If the mirror moves back in the negative ξ direction the atoms also turn left at every resonance and move to the left into the diagonal potential valley before reaching the zero potential line.

Interestingly, the radiation pressure force is different for the two distinct paths the atoms take as the mirror is moving back and forth (see Fig. 9). Hence the light field performs work on the mirror in every round trip, and this work can be fairly large. It should be noted, however, that our model is too simplistic to study this feature quantitatively. First, the assumption of adiabaticity of the atomic motion is likely to break down near the zeros of the numerator, where the atoms take a sharp turn to the right. The potential well becomes extremely shallow in this region and when the atoms fall into the other branch of the potential, both situations for which the assumption of adiabaticity of the atomic motion may not hold. If the atoms have some inertia, they could overcome the potential wall that prevents them from going over the potential hill and continue their motion on the other side. Tunneling through the barrier is another possibility. For these reasons we concentrate in the following on the case where the atoms move with the moving mirror, i.e., where the reflectivity of the moving mirror is higher than that of the fixed mirror. For this type of motion the adiabaticity assumption holds at all times.

Once the position of the atom mirror $z_a(\xi)$ has been determined we can find the radiation pressure force by inserting $z_a(\xi)$ into the expression for ϵ_4. Figure 10 shows the three different cases of low atomic reflection coefficient and high atomic reflection coefficient, as well as an empty cavity for comparison. A small atomic reflectivity broadens the resonance. Also, the peak radiation pressure force increases. As the atomic reflectivity increases the resonance becomes wider and wider and develops a broad dip in the middle. For very high atomic reflectivities adjacent resonances "collide" and give rise to an avoided crossing behavior that results in the double-peak structure of Fig. 10. The double resonances in this regime are much wider than the empty cavity resonances and the peaks are substantially higher. Also the radiation pressure force never falls off to values as low as for the empty cavity. The low-intensity region between the double peaks is the limiting shape of the aforementioned dips that develop in the resonant line shape.

From the radiation pressure force we find the total potential of the moving mirror by a simple integration and by adding the harmonic potential due to the restoring force. Figure 11 shows the total potentials, again for the three different

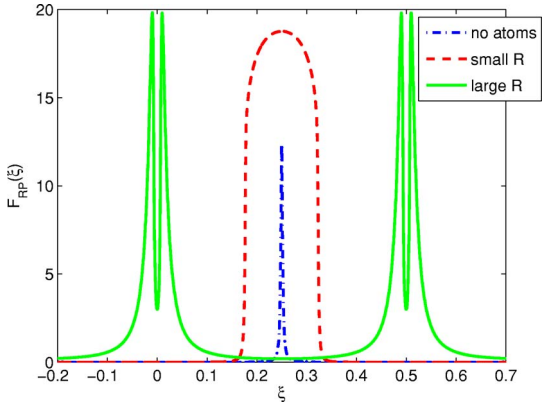

FIG. 10. (Color online) Radiation pressure force for atomic motion locked to the motion of the moving mirror for intermediate atomic transmissivity $T=0.9$ [(red) dashed line], small atomic transmissivity $T=0.05$ [(green) solid line] and an empty cavity [(blue) dash-dotted line] for comparison. To ensure that the atoms are following the desired branch of the potential we choose $T_1=0.2$, $T_2=0.1$. The injected laser power is 0.01 W and $\alpha=10$ W^{-1}.

cases considered for the radiation pressure force above. Every time the mirror moves through a resonance the potential makes a steep step down. The steps are highest if the atoms have intermediate reflectivity due to the broad and high resonances. The global minimum of the potential is near $\xi\approx 5$ in this case. They are smaller for the double peaks for high atomic reflectivity and smallest for the empty cavity.

IV. SIGNATURES OF THE COUPLED MOTION

The question of how to detect the coupled motion of the mirror and the atoms naturally arises. A possible observable is the spectrum of the light transmitted through the cavity. The amplitude and phase modulation of the optical field due to the mirror motion are detectable as sidebands in the spectrum of transmitted light.

To find the spectrum of the transmitted light we integrate the Newtonian equations of motion of the mirror subject to the modified radiation pressure force using the velocity Verlet algorithm.[4]

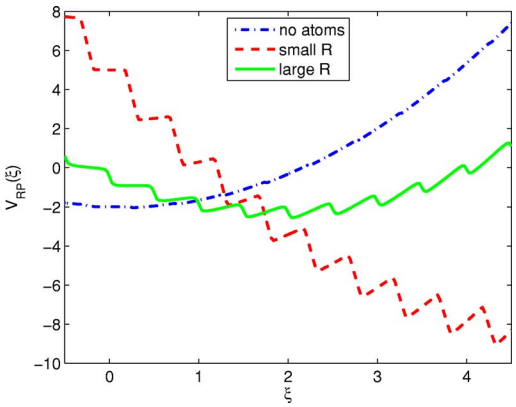

FIG. 11. (Color online) Radiation pressure potential for atoms moving with the moving mirror and an empty cavity. All parameters as in Fig. 10.

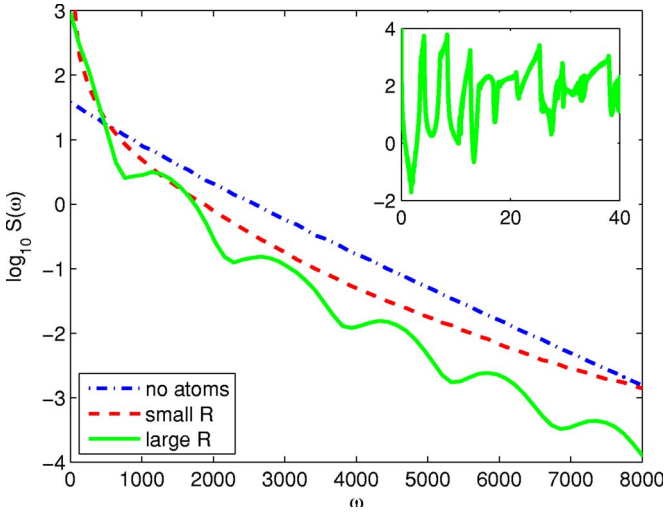

FIG. 12. (Color online) Sidebands of the transmitted light for atoms moving with the mirror, staying with the fixed mirror and for an empty cavity.

A. Large-amplitude oscillations

First we analyze what happens as the mirror undergoes large-amplitude oscillations such that in every period it sweeps over several resonances.[5] We consider again the three cases of atoms with high reflectivity and intermediate reflectivity, and an empty cavity. The cavity and atomic parameters are the same as before and as for the quality factor of the cavity we choose $\Gamma^{-1}=10^4$.

Figure 12 shows the resulting sideband spectra. For clarity each data point has been obtained by averaging over 1000 frequency bins. The spectrum of the empty cavity falls off nearly exponentially, a consequence of the near-Lorentzian line shape of the resonances and the fact that the mirror moves through each resonance at nearly constant velocity.

The widths of the transmission spectra are comparable in all three cases, confirming that the widths of the resonances

[4]The canonical nature of this algorithm is necessary because we have to integrate the equations of motion over very long time intervals, typically several ten thousand cycles. At the same time we have to integrate with high temporal resolution because the radiation pressure force is so sharply peaked. The position of the atoms is determined at every time step using Brent's method [24] in an interval centered at the atomic position of the previous time step and with a width that depends on the velocity of the mirror. This way we ensure that the atoms follow a continuous path along a potential valley without jumps to different valleys. The transmitted field at every time is easily found from ϵ_4. The sideband spectrum is found by numerically fourier transforming the field.

[5]To avoid too large velocities at the bottom of the potential, which would make an accurate numerical integration more difficult, we choose the initial conditions such that the mirror swings through roughly eight resonances. This number is not exact since the turning point on the left is typically at a resonance.

are of the same order. However, the spectra acquire a peak near $\omega=0$ for nonzero atomic reflectivities, a consequence of the larger resonance widths in these cases; in addition the light field never falls off to zero, in contrast to the empty cavity case where it does so to a good approximation for high-reflectivity mirrors. Especially for high atomic reflectivity the cavity always leaks a significant amount of light, which gives rise to an enhanced dc component in the transmission spectrum.

The fringes that appear in the case of high atomic reflectivity can be understood in the following way. Two light pulses exit the cavity whenever the mirror passes through a resonance (see Fig. 10), and they give rise to a double-slit diffraction pattern in frequency space. Their spacing corresponds to the inverse of the time it takes the mirror to travel from the first peak to the second peak of the double resonance.

The inset of Fig. 12 shows the details of the low-frequency part of the spectrum for the case of high atomic reflectivity. (The low-frequency part is similar in all cases.) It consists of a peak at the frequency corresponding to the time it takes the mirror to move from one resonance to the next and of a series of additional peaks at each harmonic. These strong components are a result of the highly nonlinear potential. The fact that the mirror moves at different speeds between different resonances gives rise to a broadening of the harmonics into bands whose width increases with growing harmonic number and which finally overlap. Effects due to the damping of the mirror motion cannot be resolved because of this broadening.

B. Small-amplitude oscillations

In our units the average thermal energy of the mirror at room temperature is $T\approx 10^{-5}$. Comparing with the energy scale in Fig. 11 we see that the mirror can undergo many oscillations in each one of the sawtooth-shaped local potential minima before it hops to a different local minimum due to thermal activation or some other perturbation. Thus it is an interesting question to determine the oscillation frequency at every local minimum for small-amplitude oscillations.

Figure 13 shows these frequencies for the three cases already discussed. For high atomic reflectivity, and in contrast to the intermediate-reflectivity and empty cavity cases, the oscillation frequency near $\xi=0$ is much lower than the restoring frequency of the mirror. This is because the resonances have wide wings in this case and, if added to the harmonic oscillator potential of the mirror, they can compensate the harmonic restoring force almost completely over a large range of displacements ξ and give rise to an extremely flat potential near the local minimum. In the other two cases the onset of the radiation pressure force near the resonances is very abrupt and the frequency of the mirror motion can never be significantly smaller than the oscillator frequency. At higher displacements from the mirror rest positions the stronger resonances found with atoms inside the cavity give rise to stronger confinement and lead to resonance frequencies that eventually become higher than in the empty cavity case. Note that for the empty cavity cases we could find only a few more local minima beyond $\xi=8$ and these could not be reasonably approximated by a harmonic potential.

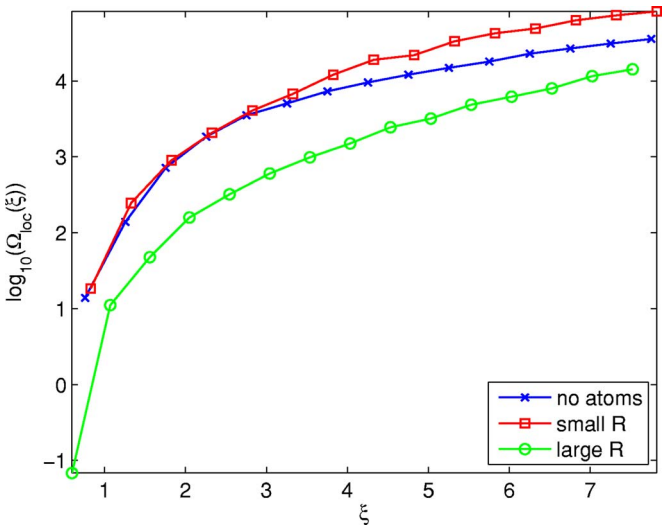

FIG. 13. (Color online) Approximate harmonic frequencies near the local minima for atoms with high reflectivity and intermediate reflectivity and an empty cavity. All parameters as in Fig 12.

V. CONCLUSION AND OUTLOOK

We have developed a model that describes the coupled motion of a cavity end mirror and atoms trapped in the standing-wave intracavity field. The key result is that the resulting model is simple enough to allow for a fairly straightforward analysis. The self-consistent electric field inside the cavity containing the atoms plays a central role since from this field we find the modified dipole potential in which the atoms move as well as the modified radiation pressure force acting on the moving mirror. We find that as a result of the strong coupling between light field and atoms due to the collective back action of the atoms the dipole potential changes qualitatively, the most notable feature being that the atomic position becomes bistable. The resonances of the cavity are broadened and develop a double-peak structure in the limit of high atomic reflectivity. We have studied the dynamics of the mirror subject to the modified radiation pressure force in the adiabatic limit where the atomic motion is much faster than the motion of the mirror and the light field is slaved to both atoms and mirror. We have shown that the sidebands of the light transmitted through the cavity can serve as an indicator of the coupled motion of the mirror and the atoms.

Many open questions remain to be studied. First of all a more careful analysis of the spatial mode structure inside the cavity in the presence of the atoms is desirable. Such an analysis could start from the Maxwell-Bloch equations and should include scattering losses due to spontaneous emission from the atomic excited state. It would yield more accurate values for the effective reflection coefficient of the atoms and the modified dipole potential, especially if R_1 and R_2 are very different.

One should also consider different adiabaticity regimes, or abandon the assumption of adiabaticity altogether. The

situation where the atomic motion is roughly as fast as the mirror motion and the atom and mirror influence each other on an equal footing is particularly interesting, and so is the case where the retardation of the light field is taken into account. Already in an empty cavity the retardation of the light field gives rise to many interesting phenomena such as instabilities, self-sustained oscillations, and chaotic behavior. It will be interesting to see how all these effects are influenced by the presence of the atoms.

A related question of practical significance is what happens if the atoms are subject to a friction force. Atoms can be efficiently cooled to very low temperatures with laser cooling and one could hope that by means of the coupling to the mirror through the cavity field one could be able to also cool the mirror. Loosely speaking, if the atoms are subject to a friction force, they lag slightly behind the position at which they ought to be according to the position of the mirror. This retardation has been seen to lead to the damping of the mirror motion in preliminary results, but these calculations need to be carried out in much more detail, especially since the momentum kicks in laser cooling, and hence the fluctuations in the atomic position, are substantial and cannot be neglected. They can be taken into account, e.g., using a master equation approach.

Finally, one needs to address the situation where all constituents of our model are quantized. Quantization of the atomic motion should allow one to study whether the resonances can be used as beam splitters, and the properties of the resulting interferometer. Also, a detailed understanding of the role of damping of the atomic motion requires a proper quantum treatment. The quantization of the mirror motion is called for in view of the experimental goal to cool it to its quantum-mechanical ground state. Finally, a quantum treatment of the light field, and especially of its fluctuations, is interesting because of the powerful methods to measure the fluctuations of the electromagnetic field. If they are linked to fluctuations of the atomic position or the mirror position, as must be expected, one could then use the light field as a powerful diagnostic tool for the study of these mechanical fluctuations.

ACKNOWLEDGMENTS

This work is supported in part by the U.S. Office of Naval Research, by the National Science Foundation, by the U.S. Army Research Office, by the Joint Services Optics Program, and by the National Aeronautics and Space Administration.

[1] A. Dorsel, J. D. McCullen, P. Meystre, E. Vignes, and H. Walther, Phys. Rev. Lett. **51**, 1550 (1983).
[2] P. Meystre, E. M. Wright, J. D. McCullen, and E. Vignes, J. Opt. Soc. Am. B **2**, 1830 (1985).
[3] S. Solimeno, F. Barone, C. de Lisio, L. Di Fiore, L. Milano, and G. Russo, Phys. Rev. A **43**, 6227 (1991).
[4] F. Marquardt, J. G. E. Harris, and S. M. Girvin, e-print cond-mat/0502561.
[5] C. Stambaugh and H. B. Chan, e-print cond-mat/0504791.
[6] B. Meers and N. MacDonald, Phys. Rev. A **40**, 3754 (1989).
[7] V. Pierro and I. M. Pinto, Phys. Lett. A **185**, 14 (1994).
[8] J. M. Aguirregabiria and L. Bel, Phys. Rev. A **36**, 3768 (1987).
[9] I. Wilson-Rae, P. Zoller, and A. Imamo$\bar{g}$lu, Phys. Rev. Lett. **92**, 075507 (2004).
[10] P. F. Cohadon, A. Heidmann, and M. Pinard, Phys. Rev. Lett. **83**, 3174 (1999).
[11] Constanze Höhberger Metzger and K. Karrai, Nature (London) **432**, 1002 (2004).
[12] D. Vitali, S. Mancini, L. Ribichini, and P. Tombesi, J. Opt. Soc. Am. B **20**, 1054 (2003).
[13] K. Jacobs, I. Tittonen, H. M. Wiseman, and S. Schiller, Phys. Rev. A **60**, 538 (1999).
[14] I. Tittonen, G. Breitenbach, T. Kalkbrenner, T. Müller, R. Conradt, S. Schiller, E. Steinsland, N. Blanc, and N. F. de Rooij, Phys. Rev. A **59**, 1038 (1999).
[15] J.-M. Courty, A. Heidmann, and M. Pinard, Eur. Phys. J. D **17**, 399 (2001).
[16] W. Marshall, C. Simon, R. Penrose, and D. Bouwmeester, Phys. Rev. Lett. **91**, 130401 (2003).
[17] L. Bel, J. L. Boulanger, and N. Deruelle, Phys. Rev. A **37**, 1563 (1988).
[18] C. K. Law, Phys. Rev. A **51**, 2537 (1995).
[19] I. H. Deutsch, R. J. C. Spreeuw, S. L. Rolston, and W. D. Phillips, Phys. Rev. A **52**, 1394 (1995).
[20] M. Greiner, O. Mandel, T. Esslinger, T. W. Hänsch, and I. Bloch, Nature (London) **415**, 39 (2002).
[21] P. Meystre and M. Sargent III, *Elements of Quantum Optics*, 3rd ed. (Springer-Verlag, Berlin, 1999).
[22] M. Born and E. Wolf, *Principles of Optics*, 6th ed. (Cambridge University Press, Cambridge, U.K., 1980).
[23] S. Slama, C. von Cube, M. Kohler, C. Zimmermann, and P. W. Courteille e-print quant-ph/0511258.
[24] W. H. Press, S. A. Teukolsky, W. T. Vetterling, and B. P. Flannery, *Numerical Recipes in C*, 2nd ed. (Cambridge University Press, Cambridge, U.K., 1992).